

# Bottom

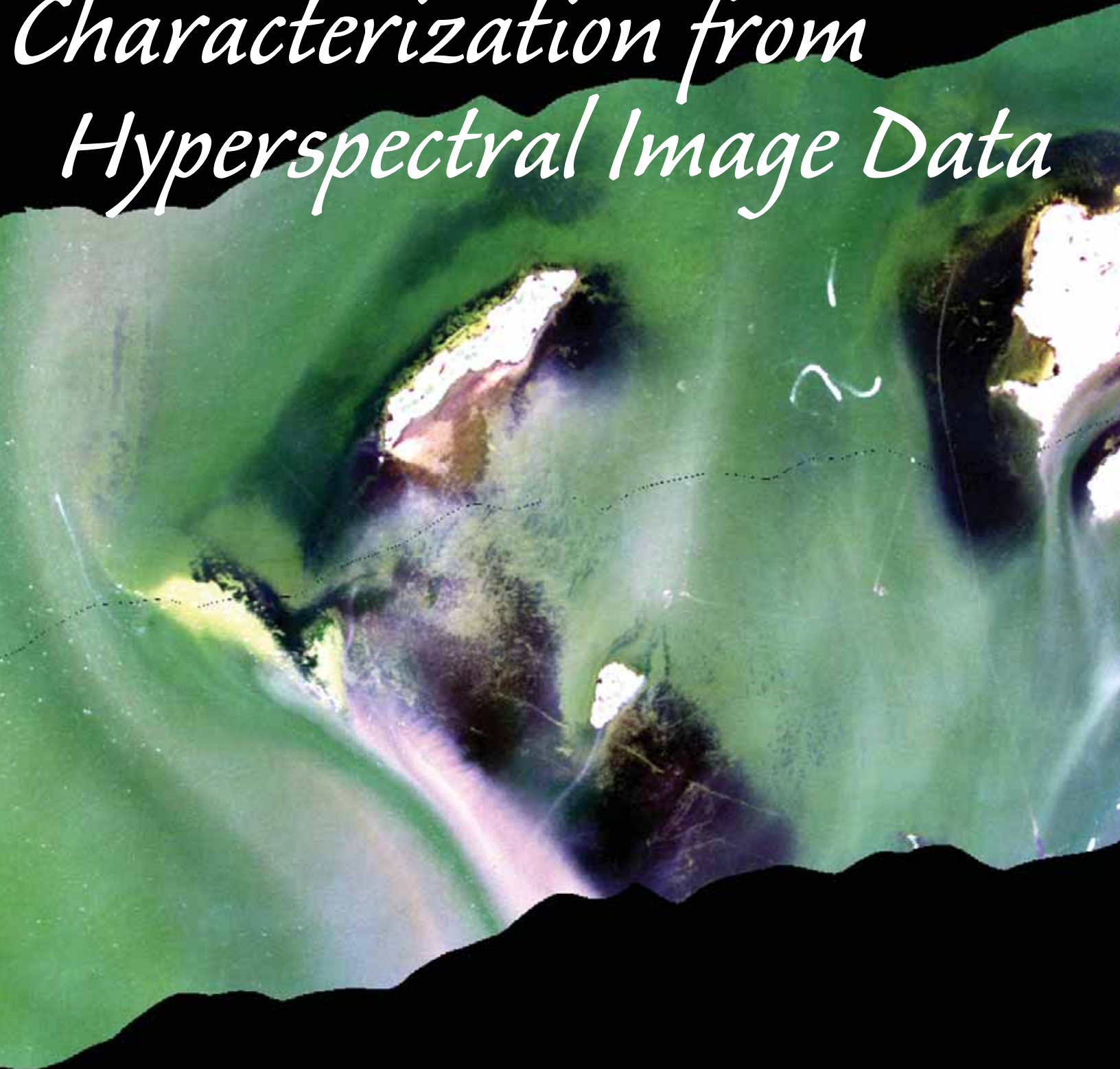
BY WILLIAM PHILPOT, CURTISS O. DAVIS,  
W. PAUL BISSETT, CURTIS D. MOBLEY,  
DAVID D.R. KOHLER, ZHONGPING LEE,  
JEFFREY BOWLES, ROBERT G. STEWARD,  
YOGESH AGRAWAL, JOHN TROWBRIDGE,  
RICHARD W. GOULD, JR., AND ROBERT A. ARNONE

## INTRODUCTION

In optically shallow waters, i.e., when the bottom is visible through the water, a tantalizing variety and level of detail about bottom characteristics are apparent in aerial imagery (Figure 1a). Some information is relatively easy to extract from true color, 3-band imagery (e.g., the presence and extent of submerged vegetation), but if more precise information is desired (e.g. the species of vegetation), spatial and spectral detail become crucial. That such information is present in hyperspectral<sup>1</sup> imagery is clear from Figure 1b, which illustrates the Remote Sensing Reflectance spectra for several selected points in the image. Spectral discrimination among bottom types will be greatest in shallow, clear water and will decrease as the depth increases and as the optical water quality degrades. Discrimination can also be complicated by the presence of vertical structure in the optical properties of the water, or even if there is a layer of suspended material near the bottom (see Box on opposite page). Despite these difficulties, bottom characterization over the range of depths accessible to remote sensing is important since it corresponds to a significant portion of the photic zone in coastal waters. Mapping bottom types at these depths is useful for applications related to habitat, shipping and recreation. The purpose of this paper is to present the issues affecting bottom characterization and to describe various methods now in use. Given space limitations, we refer the reader to the references for results and examples of bottom type maps.

<sup>1</sup>Hyperspectral imagers collect data simultaneously in dozens or even hundreds of narrow, contiguous spectral bands. This is in contrast to multispectral sensors, which produce images with a few relatively broad wavelength bands.

# *Characterization from Hyperspectral Image Data*



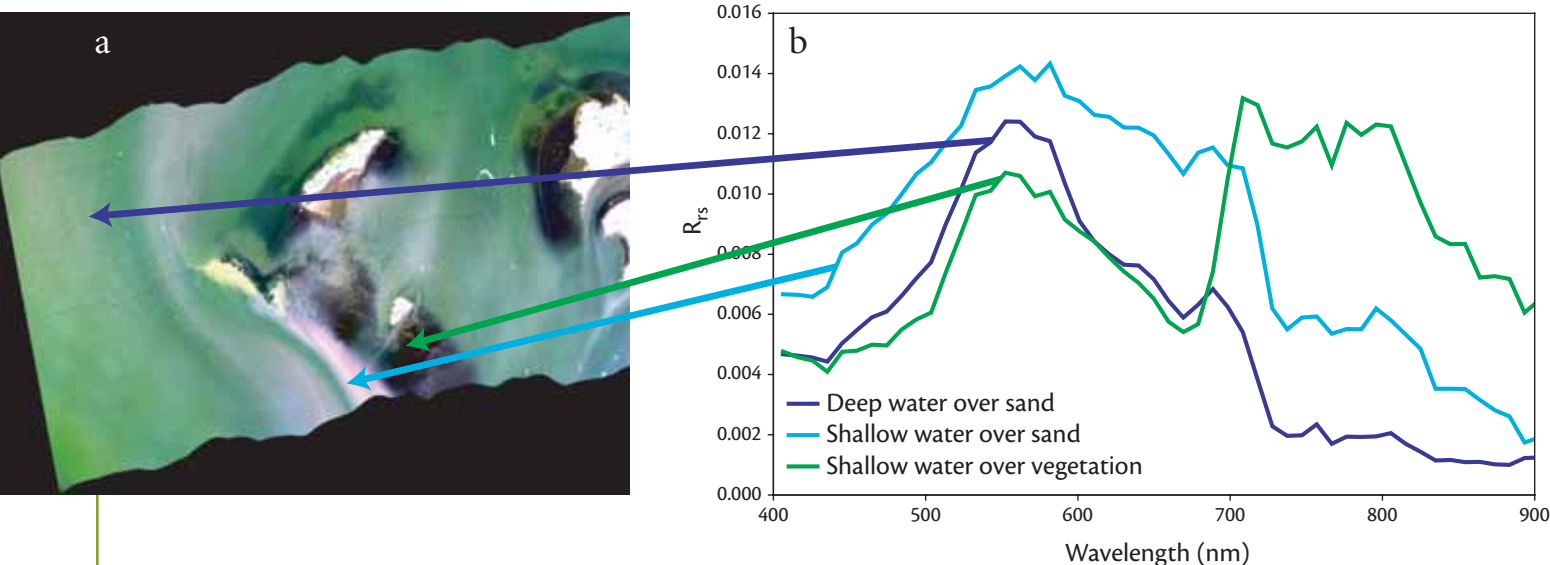


Figure 1. (a) A portion of PHILLS-1 image of an area in Barnegat Bay, New Jersey, collected on 23 Aug 2001 illustrating a variety of spectrally different bottom types. (b) Remote sensing reflectance ( $R_{rs}$ ) spectra at the water surface for selected points in (a) derived from the Portable Hyperspectral Imager for Low-Light Spectroscopy (PHILLS) data.

### UTILITY OF MAPPING IN THE COASTAL ZONE USING PASSIVE IMAGE DATA

Passive optical remote sensing (i.e., imagery from aircraft or satellite) provides one of the only viable approaches for effectively mapping coastal ecosystems. It is useful not only for delineating the extent and distribution of different bottom types, but also makes it feasible to monitor changes in habitat and dynamic systems because it is possible to revisit a site on a regular basis. Events requiring rapid response (storm events), frequent coverage (sediment transport), or periodic coverage (monitoring coral beds) can be accommodated relatively inexpensively.

Active systems that are specifically designed for bathymetric mapping are not typically very effective at distinguishing among bottom types. Acoustic systems, which are the standard for bathymetric mapping in deeper waters (>5 meters), can be adapted to make crude bottom type classifications

(Siwabessy et al., 2000). Similarly, lidar bathymetry, which is very effective in optically shallow waters where boat operations may be difficult or when rapid coverage is required (Guenther et al., 2000), is also capable of rough bottom characterization. However, passive optical imagery is much more effective for mapping bottom type wherever the bottom is visible (up to 20 meters in the clearest waters).

### PREPARING THE DATA

Extracting meaningful results from passive optical data is a two-step process. First, the data are calibrated and the atmospheric portion of the signal received at the sensor is removed, leaving the “water leaving radiance.” The water leaving radiance is typically divided by the incoming solar irradiance to produce  $R_{rs}$ , which contains all of the information about the water column and ocean

---

**William Philpot** ([wdp2@cornell.edu](mailto:wdp2@cornell.edu)) is Associate Professor, School of Civil and Environmental Engineering, Cornell University, Ithaca, NY. **Curtiss O. Davis** is at Remote Sensing Division, Naval Research Laboratory, Washington, DC. **W. Paul Bissett** is Research Scientist, Florida Environmental Research Institute, Tampa, FL. **Curtis D. Mobley** is Vice President and Senior Scientist, Sequoia Scientific, Inc., Bellevue, WA. **David D.R. Kohler** is Senior Scientist, Florida Environmental Research Institute, Tampa, FL. **Zhongping Lee** is at Naval Research Laboratory, Stennis Space Center, MS. **Jeffrey Bowles** is at Naval Research Laboratory, Washington, D.C. **Robert G. Steward** is at Florida Environmental Research Institute, Tampa, FL. **Yogesh Agrawal** is President and Senior Scientist, Sequoia Scientific, Inc., Bellevue, WA. **John Trowbridge** is Senior Scientist, Applied Ocean Physics and Engineering, Woods Hole Oceanographic Institution, Woods Hole, MA. **Richard W. Gould, Jr.** is Head, Ocean Optics Center, Naval Research Laboratory, Stennis Space Center, MS. **Robert A. Arnone** is Head, Ocean Sciences Branch, Naval Research Laboratory, Stennis Space Center, MS.

# BOTTOM NEPHELOID LAYER

BY YOGESH AGRAWAL

Quite like the dust layer that establishes itself over land under a strong wind, a particle-rich nepheloid layer typically exists on the ocean floor. The dynamics of this layer constitute the area of research called bottom boundary layers and sediment transport.

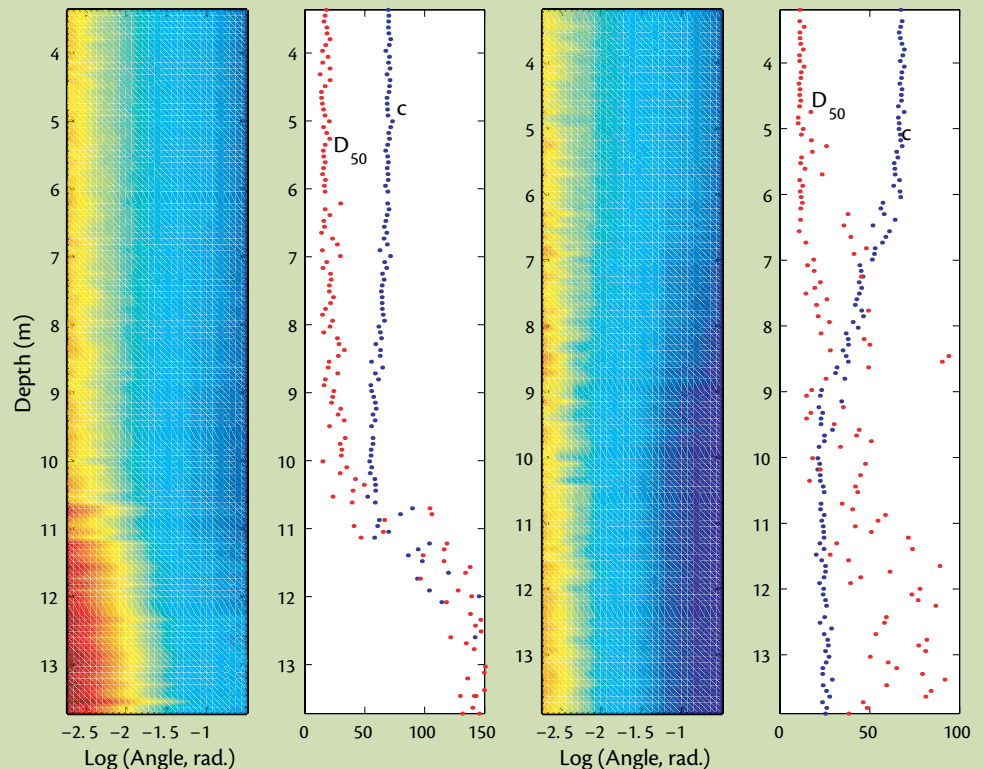
The nepheloid layer has the following four basic properties: (1) the layer has a thickness that scales with the vigor of the currents on the bottom,  $k u_* / f$ ; where  $k$  is about 0.41,  $u_*$  is the bottom friction velocity ( $=\sqrt{\tau/\rho}$ ,  $\tau$  being bottom frictional stress and  $\rho$  being water density), and  $f$  is the Coriolis parameter, (2) the water in the layer is typically most turbid at the greatest depth and clears further from the boundary, (3) the layer is sustained by a balance between gravitational settling and turbulent vertical diffusion counteracting it, and (4) there exists a vertical gradient in the concentration of particles of any given size, with the gradient being strongest for the fastest settling particles. In addition to these four basic properties, the dynamics of the bottom nepheloid layer are characterized by the stripping of sediment off the seafloor due to frictional stress of water motions so that the availability of sediment at the bed may determine the bottom boundary condition for sediments. Whereas all of these properties are similar to common atmospheric experience, waves introduce an additional phenomenon on the seafloor that has no counterpart in the atmosphere. Surface gravity waves induce oscillatory motions on the seabed. This motion, in turn has its own, typically much thinner boundary layer—a wave boundary layer—that is capable of suspending more bed material than an equally strong current. As a result, a combination of waves and currents can suspend a large amount of material. The suspended material increases the beam attenuation coefficient  $c$ . Conversely, the absence of bottom water motion permits the sediment to fall out of suspension, clearing the water column. Observations in the nepheloid

layer have been made quite extensively. These reveal a wide dynamic range of changes in the amount of sediment carried in the nepheloid layer.

From the standpoint of optics, the nepheloid layer complicates bathymetry. For example, the suspended particles reflect light from a LIDAR pulse, which stretches a bottom return. Furthermore, as light propagates into the nepheloid layer it is absorbed, so that a weaker laser pulse reaches the bottom. The bottom-reflected energy is again attenuated as it propagates through the nepheloid layer up toward the surface. This two-way attenuation depends on the beam attenuation coefficient  $c$  and the boundary layer thickness. Given typical order of magnitude values for  $c$  [ $\sim 1\text{-}30\text{ m}^{-1}$ ] and boundary layer thickness  $\delta$  of order 10 m, it is readily apparent that the round-trip attenuation of a laser pulse can reach  $\exp(-10)$  or more. Thus the presence of a

bottom nepheloid layer can dramatically influence the visibility of the bottom from above, restricting LIDAR bathymetry.

In addition to the bottom resuspension mechanism described above, other more complex processes determine the overall water column properties. For example, upwelling events can act as conveyor belts, carrying to the surface sediment that was originally present in the nepheloid layer. In such cases, a bottom and surface nepheloid layer can exist. A surface wind stress may produce thickening of the surface layer, leading to interaction of the two, and establishment of a more complex columnar turbidity structure. Needless to say, given all the factors that determine the overall properties of a water column, continuing research in the underlying processes is vital to improving our quantitative understanding. 



Two pairs of figures illustrate a case of an existing bottom turbid layer (left) versus a surface turbid layer (right) presumably due to an upwelling event. The left panel in each pair is the volume scattering function, plotted against depth on the ordinate. The right panel of each pair is a vertical profile of the beam- $c$  (attenuation) [magnified by 20x] and the mean sediment grain diameter in microns. In the turbid bottom layer case, it is the classic behavior of larger grains and larger attenuation hugging the bottom. The turbid surface layer is quite different: the beam- $c$  is higher near surface. The volume scattering function (VSF) is weaker and less steep, and the grain size is larger though more scattered in the lower half, despite lower beam- $c$ ; all these characteristics are probably due to the presence of marine flocs.

bottom. Second,  $R_{rs}$  data are analyzed to retrieve the products of interest, such as water clarity, bathymetry, and bottom types.

The Portable Hyperspectral Imager for Low-Light Spectroscopy (PHILLS; Davis et al., 2002) is a hyperspectral imager designed specifically for characterizing the coastal ocean. The main components are a high-quality video camera lens, an Offner Spectrometer that provides virtually distortion free spectral images, and a charge-coupled device (CCD) camera. The CCD camera has a thinned, backside-illuminated CCD for high sensitivity in the blue, essential for ocean imaging. The instrument is designed in such a way that each pixel across the CCD array is a different cross-track position in the image. For each cross-track position, the spectra are dispersed in the corresponding vertical column of the array. The along-track spatial dimension is built up over time by the forward motion of the aircraft yielding a three-dimensional image cube. The PHILLS imagers are characterized in the laboratory for spatial and spectral alignment, stray light and other distortions that will need to be corrected in the data. The imagers are calibrated spectrally using gas emission lamps and radiometrically using a large calibration sphere. Details of the instrument design and calibration can be found in Davis et al. (2002). Kohler et al. (2002) have developed an innovative approach for imaging the integrating sphere through a variety of colored glass filters. This approach further improves the calibration and, in particular, provides a unique approach to correct for the small

amount of residual stray light that is typical of spectrometer instruments.

Atmospheric correction is done using TAFKAA<sup>2</sup> (Gao et al., 2000; Montes et al., 2001), which is the only atmospheric correction algorithm specifically designed to correct ocean hyperspectral data. The algorithm uses lookup tables generated with a vector radiative transfer code that includes full polarization effects. An additional correction is made for skylight reflected from the wind roughened sea surface. Aerosol parameters may be determined using the near infrared wavelengths pixel by pixel for the entire scene, or for a selected region of the image. Alternatively, aerosol parameters may be input based on ancillary data collected during the experiment. Some experience is generally required in the selection of aerosol parameters, and other inputs that are appropriate for the image. In a typical experiment, the  $R_{rs}$  calculated from the calibrated and atmospherically corrected data will be checked against ship and mooring measurements to ensure a realistic result.

## INTERPRETING THE OCEAN SIGNAL

Many factors affect remotely observed water color in shallow waters. First, just as in deep water, the water itself (including dissolved and particulate material) transforms the incident sunlight and reflects part of that light back to the observer. The bottom then reflects part of the incident light in a manner that is highly dependent on the bottom material and roughness. There is no simple

way to separate water-column and bottom effects on the measured signal leaving the sea surface; however, sediments and bottom biota typically reflect more light than does a deep water body, and the reflected light is spectrally different than that of deep water, allowing scientists to obtain useful information about the bottom even in the presence of water-column effects. This is illustrated in Figure 2, which shows how water-column and bottom effects conspire to generate the upwelling radiance above the surface. As seen in Figure 2b, three bottom types (sand, grass, and black) have distinctly different spectra even when seen through the same water depth (in this case, 10 m of water).

Bottom albedo (irradiance reflectance) varies substantially among distinct bottom types (Figure 2). However, since the bottom is viewed through the water column, the useful spectral range is sharply limited by spectral attenuation by the water. In very shallow waters the useful spectral range is from ~400-720 nanometers (nm) (blue to near infrared [IR]). Because water is rather strongly absorbing in the red and infrared, the usable portion of the spectrum for bottom characterization at depths greater than a few meters is really ~400-600 nm (blue to green). This still leaves a significant range of variability due to changes in bottom albedo. Another complicating factor is that the bottom reflectance is directional (i.e., the amount of light reflected changes with both the direction of illumination and direction of view). For mathematical simplicity we frequently assume that the bottom is

<sup>2</sup>TAFKAA stands for "The Algorithm Formerly Known As ATREM", ATREM (ATmospheric REMoval) being the predecessor algorithm.

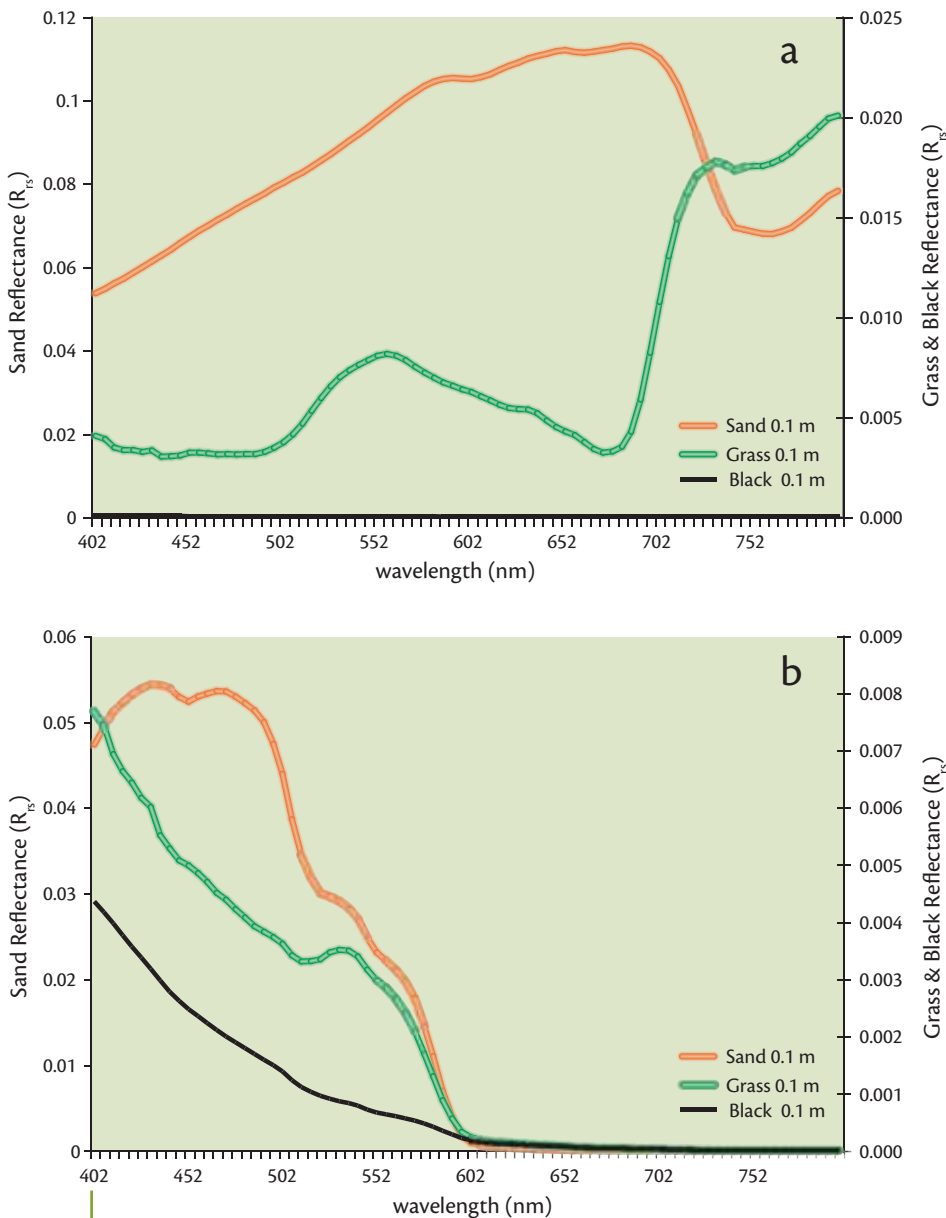


Figure 2. Remote sensing reflectance ( $R_{rs}$ ) of three different bottom types (sand, grass, and a black, non-reflective bottom) seen through clear water at depths of (a) 0.1 m and (b) 10.0 m. The spectra were simulated using Hydrolight (a radiative transfer model developed by C. Mobley, Sequoia Scientific, Inc.) In shallow water,  $R_{rs}$  is only slightly affected by the water. In deeper water, scattering and absorption by the water significantly alter the reflectance, but the spectra of the three bottom types are still distinct. Note that the non-reflective bottom is an indication of the water contribution.

Lambertian, which means that the reflected light is independent of direction. This is approximately true for at least some bottom types such as bare sand, but even where it is not, the directional dependence of the color is likely to be much less than that of the magnitude of the reflectance. In situations of practical interest, the assumption of a Lambertian bottom usually causes errors of less than ten percent in computed water-leaving radiance (Mobley et al., 2003).

In summary, there are well-proven, forward-radiative transfer models (e.g., Hydrolight, Sequoia Scientific, Inc.) that accurately describe the propagation of light through the water column, including reflection from the bottom. However, to extract information about the water and bottom optical properties from remote sensing data, an inverse model is needed. There are a number of approaches to the problem of inversion which are discussed in the next section.

## INVERSION METHODS

**Analytical Methods:** It would be ideal to have an invertible analytical model from which one could derive the bottom characteristics directly. However, due to the complexity of radiative transfer in optically shallow environments, invertible models are necessarily simplified analytical models that incorporate very limiting assumptions (Gordon and Boynton, 1997). They are usually designed for a specific data set and for operation with a minimum number of wavebands. Such models typically assume that the water is optically homogeneous and are used to solve for the depth assuming that the bottom type is uniform (Lyzenga, 1978). Although it is feasible to find a solution for the

depth that is independent of bottom type (Philpot, 1989), inversion of the analytical model requires calibration using at least two known depths over each bottom type within the scene.

**Optimization Approaches:** Passive, remote-sensing, bathymetric and bottom characterization algorithms must contend with spectral changes caused by optical properties of water (assumed to be vertically invariant), depth of the water, and bottom reflectance. These algorithms must either fix all but one parameter, or must solve for several spectral parameters simultaneously. With hyperspectral imagery as the data source, a multi-parameter model may be expressed as a set of linear equations, with one equation for each spectral band. However, since all parameters but depth are spectral, the set of equations will remain underdetermined, and the number of possible solutions is infinite. In this case, using hyperspectral data (i.e., increasing the number of spectral bands) does not help determine the system. However, the changes in adjacent bands are not independent, and the relationship between one wavelength and neighboring wavelengths can be exploited. This can be best accomplished when the number of spectral bands is sufficient to resolve the subtle spectral variations that arise when the magnitude of various components change. Additionally, using spectral derivatives in addition to the standard form allows for expansion in the number of equations without altering the number of unknowns (Kohler, 2001). This in turn expands the equation set, making the system no longer underdetermined (Lee, 1999, Lee et al., 2001). However, expanding

the equation set introduces a level of complexity in the procedure, making methods of optimizing the process necessary.

A variety of continuous and stochastic optimization techniques are available, however, determining which are the most beneficial is still an active research topic. Optimization, which by its nature is an iterative procedure, can be very time consuming. While these approaches have shown initial promise, the algorithms are still in an early stage of development.

**Look-up Tables:** Another effective technique for extracting environmental information from hyperspectral imagery is “look-up-table” (LUT) methodology, which works as follows: a radiative transfer model such as Hydrolight is used to generate a large database of  $R_{rs}(\lambda)$  spectra, which corresponds to various water depths, bottom reflectances, and water-column inherent optical properties (IOPs) for given sky and sea surface conditions and viewing geometries. This database generation is computationally expensive, but needs to be done only once. To process an image, the measured  $R_{rs}(l)$  spectrum at each pixel is then compared with the database spectra to find the closest match using a least-squares minimization. The Hydrolight input depth, bottom reflectance, and IOPs that generated the database spectrum most closely matching the measured spectrum are then taken to be the environmental conditions at that pixel. This process is illustrated in Figure 3. The current technique (Mobley et al., 2004) gives a simultaneous retrieval of both water column and bottom properties and does not require any *a priori* knowledge of the scene.

**Neural Networks:** The LUT method described above requires a large and representative set of spectra for known conditions. Given such a database, a neural network provides a purely empirical method for characterizing the seafloor or computing water depth (Sandidge and Holyer, 1998). The database is used to construct (i.e., “train”) the neural network by pairing a large number of examples of remote-sensing spectra with corresponding values of the desired property (e.g., water depth or bottom type). Because it is difficult to construct a large training set with field data, it is usually necessary to train a network with numerically simulated reflectance spectra for a randomized variety of different bottom types, water depths, water properties, and illumination conditions using Hydrolight or an equivalent radiative transfer code (Mobley et al., 1993). The resulting data set is split into two parts: a training set and a smaller testing set. The remote-sensing reflectance values of the training set are used as inputs to the neural network, with the network output being trained on one or more of the variables (e.g., water depth). During training, the same training data are passed through the network many times and the network is improved on each pass. Periodically the network is tested against the testing set, and the training stops when the performance of the network on the testing set stops improving (and begins to worsen).

When applied to real, remote-sensing data, a neural network will give the best results if the inputs used to generate the simulated training and testing sets fully cover, but do not greatly go beyond, the natural

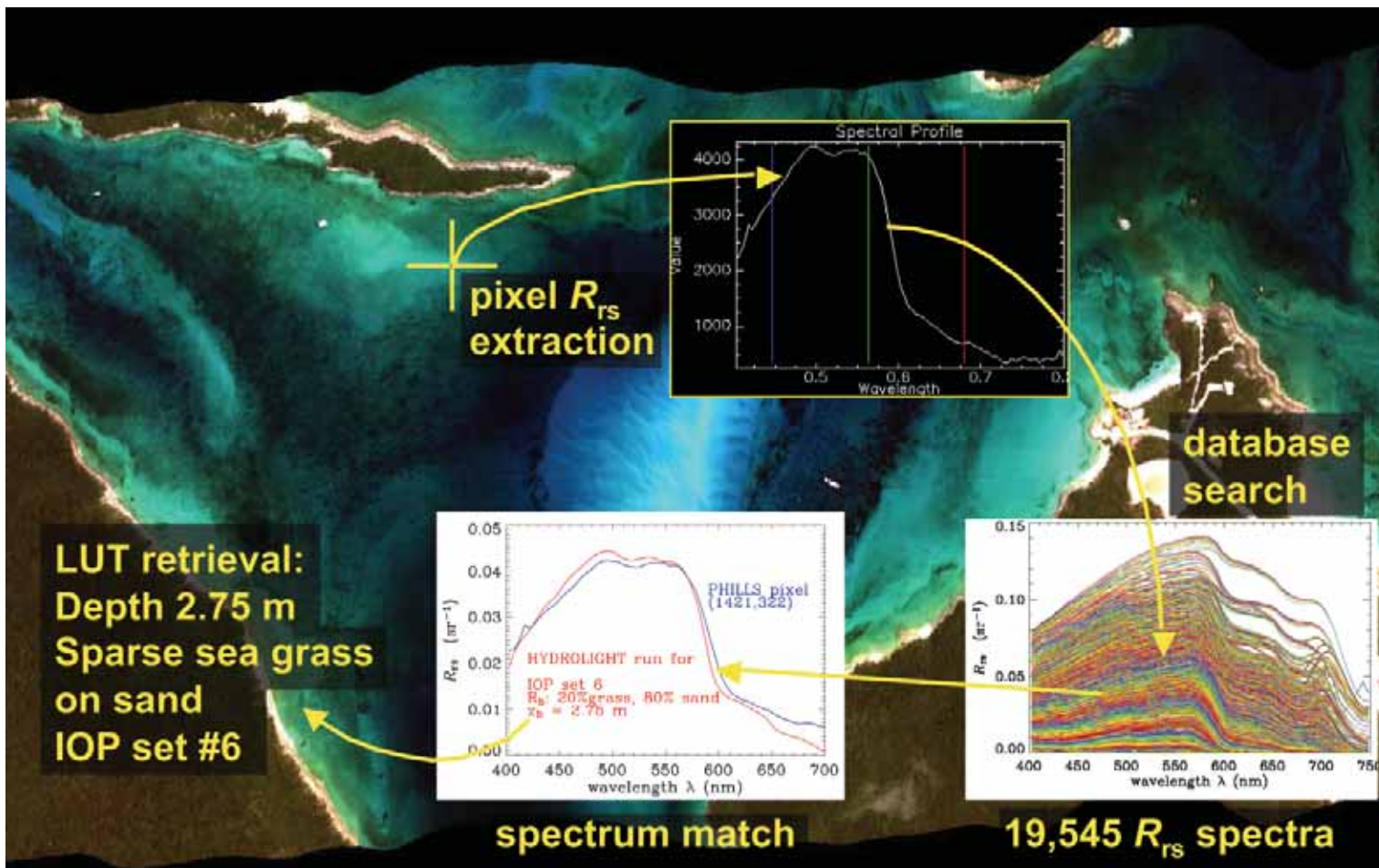


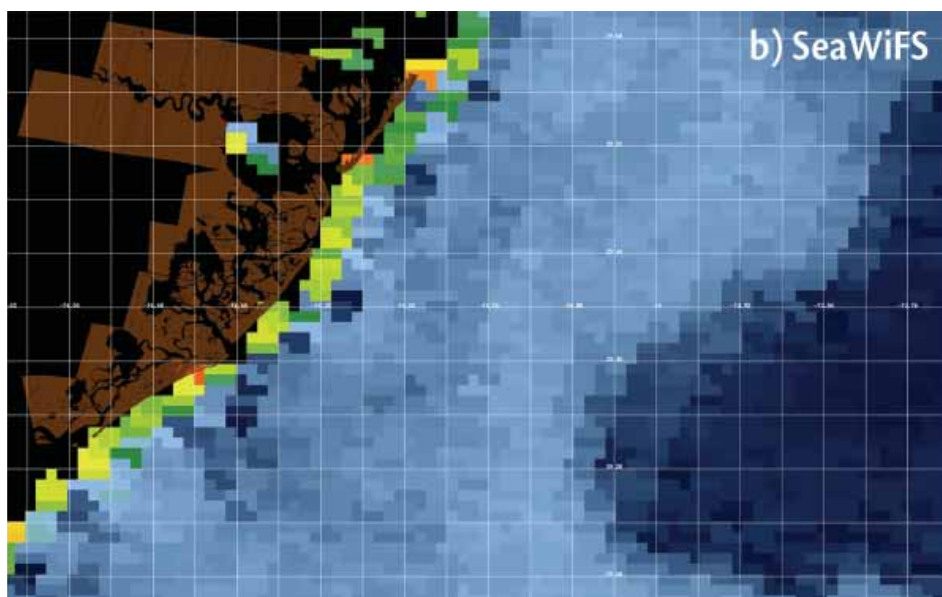
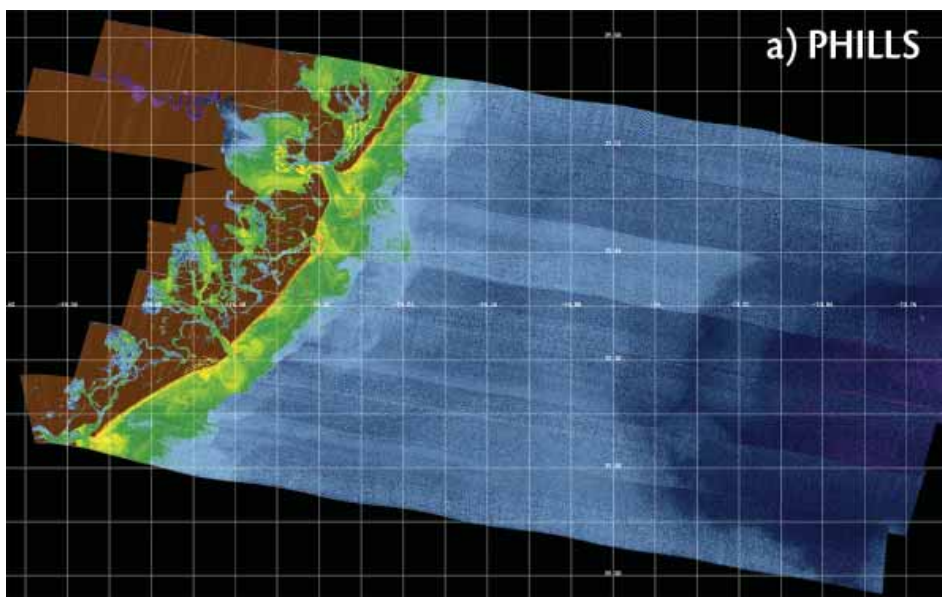
Figure 3. An image of Adderly Cut, Lee Stocking Island, Bahamas from the PHILLS hyperspectral scanner. Each pixel in the image represents the spectral remote sensing reflectance ( $R_{rs}$ ) at that point. The observed spectrum is then compared to a look-up table (LUT), a database of spectra compiled for a wide range of depths, bottom types, and water types. The depth and bottom type of the best-fit modeled spectrum is then associated with the image pixel.

variability of the site being studied. To prevent the network from learning to extract information from very small features in the remote-sensing spectra, one should add artificial noise to the simulated data before using it to train the network. The magnitude of this artificial noise should be at least as large as the noise level anticipated in real-world, remote-sensing data. Once a network is constructed for a specific region and sensor (as defined by the wavelength bands and

noise levels), no further training is necessary. A major advantage of the neural network is that once established the network can be used with very large data sets efficiently (i.e., computation time is generally not a limitation).

The contrast between the LUT and neural net methods is interesting. It is relatively easy to expand, or change the database for the LUT method, but every image spectrum must be compared with most if not all of

the spectra in the database. Performing the analysis on millions of spectra in an image can be time consuming. In contrast, with neural networks, the effort is in constructing the network. Since the network is very dependent on the specific data set used for training, it is difficult and time-consuming to change the database and retrain the network. Image analysis, however, can be accomplished in real time.



## TEMPORAL AND SPATIAL VARIABILITY

Scale issues impact both water column and bottom studies. Since the bottom is viewed through the water column with remote-sensing imagery, it is necessary to distinguish whether the signal variability observed at the sensor is due to variability in the water or to the bottom component. In general, the temporal scales of variability are longer for bottom processes than for water-column processes. The gross characteristics of the bottom do not change as rapidly as those in the water column, where fluid motion responds to the constant forcing from waves and currents. Spatial scales of variability are generally of greater importance in bottom characterization studies because temporal variations usually occur relatively slowly. In fact, steady state is often assumed for periods less than a week or two, unless a major storm alters the bottom features. Although micro- and fine-scale spatial distributions of bottom type are of ecological interest (e.g., epiphyte distributions on a single seagrass blade or within a seagrass community), the instrumentation, aircraft, and satellite remote sensors available to examine the hyperspectral character of the bottom are designed to collect data at somewhat larger scales (meters to kilometers).

In addition, issues of scale must be considered when comparing *in situ* and remotely sensed measurements, and when comparing remotely sensed measurements from sensors with different spatial resolutions. How close in time were the measurements collected? Do the measurements contain information from the same area? For example, when a spot on the ground is

Figure 4. Comparison of backscatter ( $b_b$ ) at 555 nm derived from airborne and satellite imagery of the LEO-15 study site along the coast of southern New Jersey on July 31, 2001: (a) a mosaic of high-spatial-resolution (10 m Ground Sample Distance [GSD]) imagery from the airborne PHILLS sensor and (b) low-spatial-resolution (1000 m GSD) imagery from the SeaWiFS satellite. The images cover the same region and are mapped to the same grid. The land end of the PHILLS 2 flight lines are shown in brown on the SeaWiFS image for orientation.

observed with a 10 cm field-of-view *in situ* instrument, a 2 m field-of-view aircraft sensor, and a 30 m field-of-view satellite sensor, how much of the observed variability is simply a result of the differing resolutions (i.e., subpixel variability)? Thus, issues of spatial resolution go hand-in-hand with issues of spatial variability; one must employ the proper measurement tools and analysis techniques to match the processes and scales of interest. To illustrate this concept, coincident PHILLS and SeaWiFS imagery are compared in Figure 4. These images represent the backscatter coefficient at 555 nm derived from the  $R_{rs}$  (after calibration and atmospheric correction) using the same semi-analytical backscatter algorithms. The hyperspectral PHILLS spectral channels were combined to match the SeaWiFS (Casey et al., 2001). These algorithms do not account for the influence of bottom reflectivity and assume optically deep water. However, note that an identical color table has been applied and very similar values of the backscatter coefficient are shown for both images from two separate sensors. This suggests that the calibration and atmospheric correction are correct; so, the in-water algorithms retrieve almost coincident backscattering values for the two different sensors. Given these identical retrieved values, we can illustrate that the increase spatial resolution (10 m) from PHILLS is required in coastal waters to resolve the changing optical conditions. Not only does SeaWiFS lack the spectral resolution to characterize bottom types (as discussed above; it has only eight spectral channels), but also the one-kilometer pixel size precludes it from resolving many coastal features readily apparent in the ten-meter-resolution hyperspectral PHILLS imagery.

## SUMMARY

Although difficulties clearly remain, the capacity for characterizing bottom types in optically shallow waters is feasible. It is also clear that hyperspectral data are best suited for meaningful and consistent classification of bottom types, especially in the presence of spatial variability in optical water quality. In this paper, we have demonstrated bottom classification using a number of data analysis tools. Such tools may prove essential for monitoring an increasingly dynamic and endangered coastal zone.

## ACKNOWLEDGMENTS

This research was supported by the Office of Naval Research. 

## REFERENCES

- Casey, B., R.A. Arnone, P. Martinolich, S.D. Ladner, M. Montes, D. Kohler, and W.P. Bissett, 2002: Characterizing the optical properties of coastal waters using fine and coarse resolution. In: *Proc. Ocean Optics XVI*, Santa Fe, NM.
- Davis, C.O., J. Bowles, R.A. Leathers, D. Korwan, T.V. Downes, W.A. Snyder, W.J. Rhea, W. Chen, J. Fisher, W.P. Bissett, and R.A. Reisse, 2002: Ocean PHILLS hyperspectral imager: design, characterization, and calibration. *Optics Express*, 10(4), 210-221.
- Gao, B.-C., M.J. Montes, Z. Ahmad, and C.O. Davis, 2000: An atmospheric correction algorithm for hyperspectral remote sensing of ocean color from space. *Appl. Opt.*, 39(6), 887-896.
- Gordon, H.R., and G.C. Boynton, 1997: Radiance irradiance inversion algorithm for estimating the absorption and backscattering coefficients of natural waters: homogeneous waters. *Applied Optics*, 36(12), 2,636-2,641.
- Guenther, G.C., A.G. Cunningham, P.E. LaRocque, and D.J. Reid, 2000: Meeting the accuracy challenge in airborne lidar bathymetry. In: 20th EARSeL Symposium: Workshop on Lidar Remote Sensing of Land and Sea, Dresden, Germany. European Association of Remote Sensing Laboratories.
- Kohler, D.D.R., 2001: *An Evaluation Of A Derivative Based Hyperspectral Bathymetric Algorithm*. Dissertation, Cornell University, Ithaca, NY, 113 pp.
- Kohler, D.D.R., W.P. Bissett, C.O. Davis, J. Bowles, D. Dye, R. Steward, J. Britt, M. Montes, O. Schofield, and M. Moline, 2002: High resolution hyperspectral remote sensing over oceanographic scales at the Leo 15 Field Site. In: *Proc. Ocean Optics XVI*, Santa Fe, NM.
- Lee, Z.P., K.L. Carder, C.D. Mobley, R.G. Steward, and J.S. Patch, 1999: Hyperspectral remote sensing for shallow waters: 2. Deriving bottom depths and water properties by optimization. *Appl. Opt.*, 38(18), 3,831-3,843.
- Lee, Z.P., K.L. Carder, R.F. Chen, and T.G. Peacock, 2001: Properties of the water column and bottom derived from Airborne Visible Infrared Imaging Spectrometer (AVIRIS) data. *J. Geophys. Research*, 106(C6), 11,639-11,651.
- Louchard, E.M., R.P. Reid, C.F. Stephens, C.O. Davis, R.A. Leathers, and T.V. Downes, 2003: Optical remote sensing of benthic habitats and bathymetry in coastal environments at Lee Stocking Island, Bahamas: a stochastic spectral classification approach. *Limnol. Oceanogr.*, 48(1), 511-521.
- Lyzenga, D.R., 1978: Passive Remote Sensing Techniques For Mapping Water Depth and Bottom Features. *Appl. Opt.*, 17(3), 379-383.
- Mobley, C.D., B. Gentili, H.R. Gordon, Z. Jin, G.W. Kattawar, A. Morel, P. Reinersman, K. Stamnes, and R.H. Stavn, 1993: Comparison of numerical models for computing underwater light fields. *Appl. Opt.*, 32, 7,484-7,504.
- Mobley, C.D., H. Zhang, and K.J. Voss, 2003: Effects of optically shallow bottom on upwelling radiances: Bidirectional reflectance distribution function effects. *Limnol. Oceanogr.*, 48(1, part 2), 337-345.
- Montes, M.J., B.-C. Gao, and C.O. Davis, 2001: New algorithm for atmospheric correction of hyperspectral remote sensing data, in Geo-Spatial Image and Data Exploitation II, In: Proceedings of the SPIE, v 4383, W.E. Roper, ed, 23-30.
- Philpot, W.D., 1989: Bathymetric mapping with passive multispectral imagery. *Appl. Opt.*, 28(8), 1,569-1,578.
- Sandidge, J.C., and R.J. Holver, 1998: Coastal bathymetry from hyperspectral observations of water radiance. *Rem. Sens. of Env.*, 65, 341-352.
- Siwabessy, P.J.W., J.D. Penrose, D.R. Fox, and R.J. Kloser, 2000: Bottom Classification in the Continental Shelf: A Case Study for the North-west and South-east Shelf of Australia. In: Australian Acoustical Society Conference, Joondalup, Australia.